BMC Genomics

RESEARCH

Open Access

Transcriptomic analysis of *Virescentia guangxiensis* (Rhodophyta: Batrachospermales) revealed differential expression of genes in gametophyte and chantransia life phases

Weinan Guo[1], Fangru Nan[1], Xudong Liu[1], Qi Liu[1], Jia Feng[1] and Shulian Xie[1*]

Abstract

Background The genus *Virescentia* is a significant member of the Batrachospermaceae, exhibiting distinctive life history characteristics defined by alternating generations. This group of taxa has specific environmental requirements for growth. This paper investigates *Virescentia*, which primarily thrives in freshwater environments, such as streams and springs, characterized by low light, low temperatures, and high dissolved oxygen levels. Currently, no laboratory simulations of their growth conditions have been reported in culture studies. Additionally, previous studies indicate that comparisons of photosynthetic strength across different life-history stages of the same species have not been conducted, mainly due to the challenges of simultaneously collecting algal strains at both life-history stages.

Results During the gametophyte stage, the chloroplast and mitochondrial genomes were measured at 184,899 bp and 26,867 bp, respectively. In the chantransia stage, the lengths of these genomes were 184,887 bp and 27,014 bp, respectively. A comparison of organellar genome covariation and phylogenetic reconstruction revealed that the chloroplast and mitochondrial genomes across different life history stages were highly conserved, with genetic distances of 0 and nucleotide variants of only 9–15 bp. The mitochondrial genome of gametophyte SXU-YN24005 was found to lack two tRNA-Leu (tag) genes compared to that of the chantransia strain. Additionally, a comparative analysis of KEGG pathway transcriptome data from the two life history stages showed that 33 genes related to the ribosomal pathway and 53 genes associated with the photosynthesis pathway exhibited a significant decline in expression during the gametophyte stage compared to the chantransia stage.

Conclusion In this study, two samples of the same species at different life-history stages were collected from the same location for the first time. The analysis revealed a high degree of conservation between their organelle genomes. Additionally, transcriptome sequencing results indicated substantial differences in gene expression patterns between the two life-history stages. This research will provide reliable data to support the future histological database of freshwater red algae and will establish a theoretical basis for conserving rare and endangered species.

Keywords Freshwater red algae, *Virescentia guangxiensis*, Different life history, Organellar genome, Transcriptome analysis

*Correspondence:
Shulian Xie
xiesl@sxu.edu.cn
[1] School of Life Science, Shanxi Key Laboratory for Research and Development of Regional Plants, Shanxi University, Taiyuan 030006, China

Background

Freshwater red algae are a significant group within the ecosystems of springs and streams, playing a crucial role in maintaining ecological balance. They are also considered essential for understanding the origin and

evolution of photosynthetic eukaryotes [1–3]. Freshwater red algae have specific habitat requirements, thriving in low-light, low-temperature, and high-dissolved-oxygen environments, often forming small, isolated populations. They are primarily found in pristine, flowing streams and springs [3, 4]. The specific and complex habitats of freshwater red algae render them vulnerable to impaired growth in response to changes in the external environment. As a result of increasing global water pollution, suitable habitats for freshwater red algae in springs and streams are becoming increasingly scarce. Consequently, some groups of freshwater red algae have been classified as rare and endangered species. Therefore, it is essential to conduct relevant biological research without delay.

The genus *Virescentia*, belonging to the Batrachospermaceae (Rhodophyta, Batrachospermales), is a representative group of freshwater red algae. The life history consists of two key stages: the gametophyte and chantransia stages. Although these two stages are crucial for research, it is not easy to collect the corresponding algal strains at the same time and clarify the relationship between them, mainly due to the unique morphological characteristics of the two stages. Observations and descriptions of the morphology of these stages can enhance our understanding of the life history processes and alternation of generation.

The life history of *Virescentia* comprises two distinct modes of reproduction: sexual and asexual. In this life history, the gametophyte is the dominant stage. Under favorable conditions, haploid gametophyte undergo sexual reproduction, producing carpogonia and spermatia. The spermatium lack mobility and flagella, relying on water currents to attach to the carpogonium. After fertilization, the carpogonium germinates at the base, forming radial gonimoblast filaments that develop into globular carposporophytes. The cells at the apex of the gonimoblast filaments give rise to carposporangia that contain carpospores. Under favorable conditions, the carpospores undergo further germination, producing chantransia. The apical cells of these chantransia undergo meiosis, producing haploid gametophyte. Both the gametophyte and chantransia can reproduce asexually, producing monosporangia. This summarizes the life history of *Virescentia* and its alternating generations (Fig. 1) [4].

Molecular phylogenetic analyses based on single genes are prevalent in the Batrachospermaceae, effectively addressing taxonomic challenges arising from morphological similarities among various taxa. The emergence of high-throughput sequencing technology, along with the reduction in sequencing costs, has resulted in greater utilization of genomic, transcriptomic, and metabolomic studies in animals and higher plants. Histological studies on algae, particularly red algae, are limited compared to those on higher plants. Most studies focus on marine red algae, while research on freshwater red algae is still in its early stages [5, 6]. Nan et al. [5] investigated the differential expression of photosynthesis related genes in *Sheathia arcuata* (currently as synonym of *Sheathia longipedicellata*) under different light conditions. Their findings indicated that the photosynthesis related pathway was significantly up regulated in low light conditions. Moreover, Nan et al. [6] examined the expression

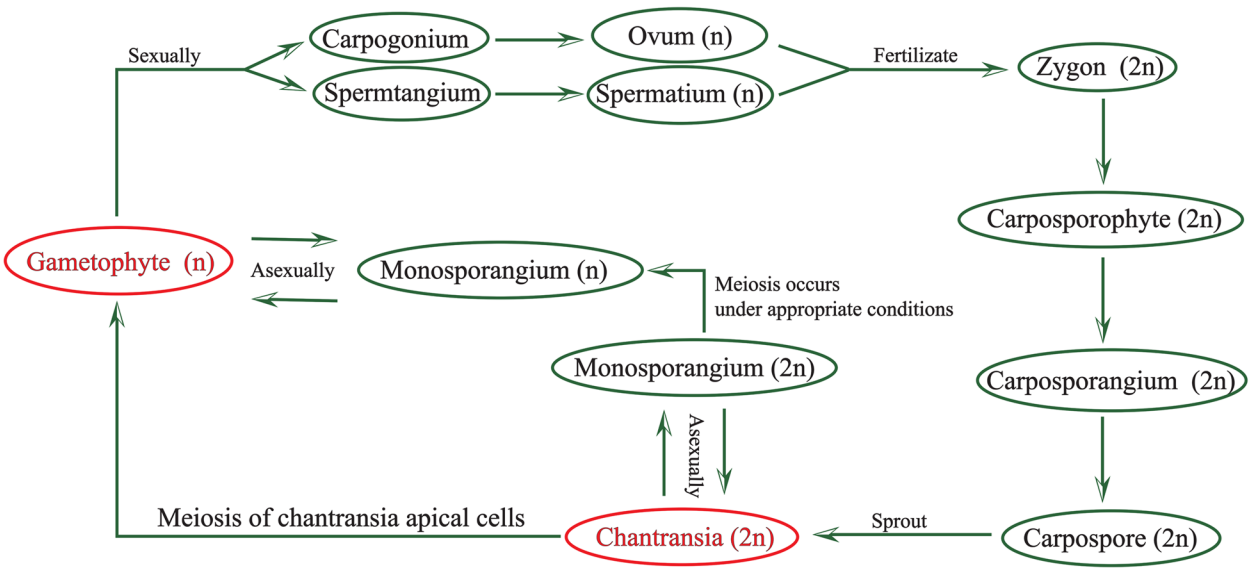

Fig. 1 Life history diagram of the Batrachospermales taxon

of differentially regulated genes across various life history stages of *Thorea hispida*.

In this study, two morphologically distinct algal strains were collected from the same location concurrently. Phylogenetic analyses of the organelle genomes revealed that these algal strains belong to the same species, *Virescentia guangxiensis*, yet represent different life history stages. Furthermore, a systematic comparison of differentially expressed genes in the transcriptomes of the two life history stages was conducted using high throughput sequencing. This research will aid in elucidating the molecular mechanisms underlying the alternating life history of freshwater red algae and establish a crucial theoretical foundation for their adaptive mechanisms in specific habitats.

Materials and methods

Sample collection

The algal strains used in this experiment were collected by Fangru Nan and Qi Liu on May 15, 2024, from Leju Village, Kunming, Yunnan Province, China (25°5′33.972″N, 102°30′39.186″E) (Fig. S1). Initially, the algal bodies were observed with an OLYMPUS SZX7 microscope. Subsequently, ultrapure water was drawn using a rubber-tipped burette to eliminate surface impurities. The cleaned algae were then divided into four sections. The first section was used to observe morphological features in vivo and was fixed in a 4% formaldehyde solution. The second section was cryopreserved at -80 °C for organelle genome sequencing. The third section was preserved in RNA Later for transcriptome sequencing. Finally, the fourth section was prepared as a specimen and deposited in the Shanxi University Herbarium (SXU).

Morphological observation

The initial step involved documenting the macroscopic morphology of the algal bodies with a digital camera (DP72). Subsequently, a portion of the fresh algal body was sampled, and its micro-morphology was photographed with a light microscope (Olympus BX-53, Olympus, Japan) (Fig. 2).

Organelle genome sequencing, assembly and annotation

Initially, the -80 °C cryopreserved algal samples were dispatched to Beijing Novozymes Technology Corporation for high-throughput sequencing. Total DNA was extracted using the protocol outlined by Saunders, incorporating modifications suggested by Vis and Sheath [7, 8]. The extracted DNA samples were tested for quality to ensure their suitability before being sequenced using the Illumina HiSeq 2500. Finally, quality control of the sequencing results was performed, including the removal of low-quality reads and the application of filtering processes to obtain high-quality clean data [9–11]. Two software programs, Price [12] and SPAdes v. 3.10.0 [13], were implemented in a Linux environment to assemble the organelles using reference genome data. This approach enabled the researchers to obtain the complete structure of the organelle genome.

Subsequently, open reading frames (ORFs) were identified, and protein-coding sequences were annotated with the Unipro UGENA v. 40 [14]. Ribosomal RNA (rRNA) positions were predicted by comparing them to published red algal relatives, while transfer RNA (tRNA) and transfer-messenger RNA (tmRNA) positions were analyzed with ARAGORN software [15]. The completed genome was subsequently circularly mapped using the OGDRAW online tool (http://chlorobox.mpimpgolm.mpg.de/OGDraw.html), and the organelle genome data from the algal samples were uploaded to the GenBank database.

Organelle genome synteny analysis

The annotated chloroplast and mitochondrial genomes of gametophyte SXU-YN24005 and chantransia SXU-YN24006 were aligned in Mauve v. 2.3.1 under the progressive mode [16]. This software facilitated the comparative analysis of the genomes.

Organelle genome phylogenomic analysis

Organelle genome sequences for each Class of the Rhodophyte were retrieved from the GenBank database. After screening, 58 chloroplast genomes and 57 mitochondrial genomes were combined with the genomic data from this study to construct a genome level phylogenetic tree (Tables S1 and S2).

Common genes were extracted from all retrieved chloroplast and mitochondrial genomes using PhyloSuite v. 1.2.3 [17]. Shared genes were concatenated by comparing and trimming multigene sequences using the MAFFT v. 7.3 [18] and the trimAl v. 1.4 [19] in PhyloSuite. Modelfinder [20] was subsequently used to identify the optimal sequence evolution model, and the Maximum Likelihood (ML) tree was constructed using IQ-TREE v. 1.6.8 [21]. This tree was analyzed with MrBayes v. 3.2.6 [22] to construct a Bayesian inference (BI) tree. Phylogenetic analyses of organelle genomes were performed.

Transcriptome sequencing and analysis

Total RNA was extracted from three gametophyte samples and three chantransia samples using the method established by Holmes and Bonner [23]. Prior to extraction, the samples were treated with RNA Later solution to prevent degradation of RNA and were subsequently stored at -80 °C. RNA integrity was assessed using 1% agarose gel electrophoresis, while RNA purity was

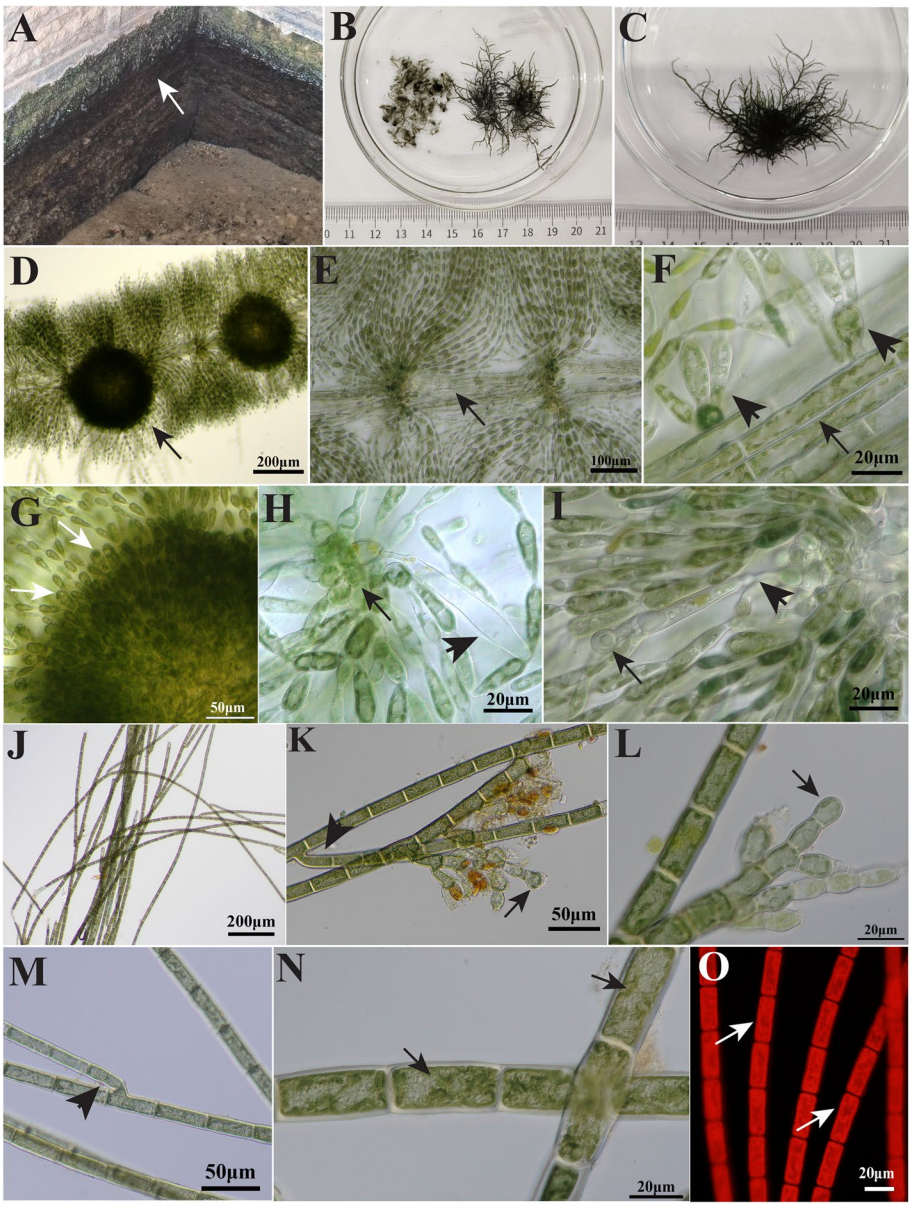

Fig. 2 Morphological character of the specimens (SXU-YN24005 and SXU-YN24006) in this study. **A** Specimens collected the stone wall of the Washing Vegetable Pool in Kunming City, Yunnan Province, China; **B** Morphology of whole thallus of chantransia specimen (left) and gametophyte specimen (right), olive-green in both stages; **C** the habit of gametophyte thallus; **D** Main axis with confluent whorls containing spherical and unstalked carposporophytes (long arrow), one per whorl; **E** Cortical filament cells (long arrow); **F** Cortical filament cells (long arrow) and secondary fascicles abundant, dichotomously or trichotomously branched, covering the entire internode; **G** gonimoblast filaments with carposporangia (white long arrow); **H** Mature carpogonium with pedicellate trichogyne (arrow) and carpogonial branches helically twisted, arising from pericentral cells (long arrow); **I** Fertilized carpogonium with clavate trichogyne (arrow) and attached spermatatangia (long arrow); **J** Micromorphology of prostrate filament; **K** Monosporangia small and abundant, ovoid or sub-spherical in shape (long arrow) and Vegetative cylindrical, fascicles branch angles ≤ 25°(arrow); **L** Monosporangia branch with ovoid or sub-spherical monosporangia (long arrow); **M** Vegetative cylindrical, fascicles branch angles ≤ 25°(arrow); **N**–**O** Cells have irregular lobed chromatoplast (white long arrow)

determined with Nanodrop spectrophotometry. Initial quantification was performed using a Qubit 2.0 Fluorometer, and the sample RNA concentration was subsequently diluted to 1.5 ng/μL. A more precise RNA integrity assay was conducted using an Agilent 2100 Bioanalyzer. The resulting mRNAs were randomly fragmented with divalent cations in NEB Fragmentation Buffer. Subsequently, the mRNA library was constructed

following the protocol outlined in the NEBNext® UltraTM RNA Library Prep Kit. Sequencing was performed using the Illumina HiSeq 2500 platform after library approval. Three biological replicates were performed for each gametophytic and chantransia stage of the algal strains, resulting in six samples for subsequent analyses.

Clean reads data from the transcriptome were assembled using Trinity v. 2.4.0 [24], and the number of reads from the compared transcripts and their expression patterns were analyzed with Corset v. 1.05 [25]. The unigenes obtained through hierarchical clustering will undergo further analysis. To obtain comprehensive gene function information, gene function annotation was conducted using seven databases. NR (NCBI non-redundant protein sequence) annotation was conducted using Diamond v. 2.1.6 [26], with a set e-value threshold of 10^{-5}. NCBI Blast 2.2.28 + [27] was utilized for NT annotation, with an e-value threshold of 10^{-5}. KOG (euKaryotic Ortholog Groups) annotation was performed with Diamond v. 2.1.6 [26], with an e-value threshold set at 10^{-3}. The Swiss-Prot database, which contains manually annotated and revised protein sequences, also employs Diamond v. 2.1.6 [26] with an e-value threshold of 10^{-5}. KEGG (Kyoto Encyclopedia of Genes and Genomes) annotations were performed using KAAS [28], with an e-value threshold of 10^{-10}. GO (Gene Ontology) annotation, conducted with Blast2GO v. 2.5 [29], with an e-value threshold of 10^{-6}. PFAM (Protein Structure Domain Annotation Database) annotation was established using hmmscan [30, 31], in the HMMER 3.0 software package with an e-value set to 0.01.

Quantification of gene transcription levels and differential transcription analysis

In this study, the gene expression levels of six samples were quantified using RSEM software [32]. Subsequently, differential transcription analysis of the gene expression levels was performed using DESeq [33] to evaluate the six samples. Based on transcriptome sequencing results, cluster analysis, GO enrichment analysis, and KEGG enrichment analysis were conducted for the differentially expressed genes, using chantransia algal strains as controls for the gametophytic strains. To minimize false positives, padj was used to adjust the P-value in hypothesis testing. A significance threshold of $|\log2(\text{FoldChange})| \geq 1$ and $\text{padj} \leq 0.05$ was established.

GO enrichment analysis

The Gene Ontology (GO) database provides comprehensive descriptions of gene functions (http://www.geneontology.org/). In this study, GO enrichment analysis was conducted using the GOseq method [34], which is based on the Wallenius non-central hypergeometric distribution. This method evaluates gene length preferences and calculates the probability of GO term enrichment by differentially expressed genes with improved accuracy. The significance threshold for GO enrichment analysis was established at $\text{padj} \leq 0.05$.

KEGG enrichment analysis

The Kyoto Encyclopedia of Genes and Genomes (KEGG) is a comprehensive database that facilitates the systematic analysis of metabolic pathways, gene product functions, and their associated compounds in cells (http://www.genome.jp/kegg/) [35]. In this study, KOBAS software [36] was utilized to analyze the KEGG functional enrichment of differentially expressed gene sets, following hypergeometric distribution principles. Moreover, the significance threshold for KEGG pathway enrichment was set at $\text{padj} \leq 0.05$.

Quantitative real-time PCR (qRT-PCR) validation

To validate the accuracy of the transcriptome results, this study selected one notable gene from each of the four significantly down-regulated pathways and confirmed these findings using quantitative reverse transcription polymerase chain reaction (qRT-PCR). Three differentially expressed genes (DEGs) related to photosynthesis were identified: LHCA1 (light-harvesting complex I chlorophyll a/b binding protein 1), *psb*O (photosystem II oxygen-evolving enhancer protein 1), and *rbc*S (ribulose-bisphosphate carboxylase small chain). Furthermore, DEG S17e (small subunit ribosomal protein S17e) was identified as involved in ribosome assembly and structural maintenance. The primers for each gene examined in this study are detailed in Table 1. ACTB served as an internal reference gene to confirm the transcriptome results for the selected genes.

Results

Morphological characteristics and identification of algal strains

This study systematically examined the morphological characteristics of the samples, with results presented in Fig. 2. During the chantransia stage, the thalli displayed

Table 1 Amplification primers used for qPCR of each gene

gene	forward primer	reversed primer
LHCA1	TTGCCACCAGTCTGCTACAG	GCTTGCGGACAGGTCTAGTT
*psb*O	CTGGATGCTAAGGGCCCAAT	CAAGAAAGAGGAGCCACGGT
*rbc*S	AACATAGAGGCCACCTGCAC	TGAGATTGACAACGCCACCA
S17e	GCCAAGGTGCTTGAGGAGAT	GGACTTCACCCAGAACTCCG
ACTB	ACTTGGCCATCAGGAAGCTC	CACAACAACTGCTGAACGGG

an olive green coloration (illustrated on the left side of Fig. 2B). Their structure comprised prostrate and erect filaments, with branching angles not exceeding 25°, exhibiting dense clumping characteristics. The vegetative cells were cylindrical and contained monosporangia with ovoid or subglobose ends at the branch terminus. Additionally, the distribution of chromatoplast cells showed laminar or irregular absences.

In the gametophyte stage, the thalli are also olive green (Fig. 2B, right side) and are relatively rich in gelatinous content, displaying an irregular branching form. The whorls were well developed, displaying a bulbous or spherical shape, and were either adjacent or separate. Secondary branches encompass the entire internode and display either dichotomous or trichotomous branching patterns.The cortical filaments are abundant and consist of one type of cylindrical cell. The primary fascicles are characterized by a straight trajectory and display dichotomous or trichotomous branching patterns. Spermatangia are typically spherical or subglobose and exist as single or binate structures. Trichogynes are characterized by a club-shaped structure with long stalk. Carpogonial branches arise from pericentral cells and take on a helically twisted configuration, embedding the carposporophyte within the whorl. Each whorl node contains a single carposporophyte.

Genomic characterisation of gametophyte and chantransia

The chloroplast genome measured 184,899 bp in length, with a GC content of 28.20% during the gametophyte period. A total of 235 genes were annotated in this genome, including 200 protein-coding genes, 31 tRNA genes, one tmRNA gene, and three rRNA genes. Additionally, the mitochondrial genome measured 26,867 bp in length and exhibited a GC content of 27.19%. A total of 47 genes were annotated in this genome, including 26 protein-coding genes, 19 tRNAs, and 2 rRNAs (Fig. 3A and B). During the chantransia stage, the chloroplast genome measured 184,887 bp in length, with a guanine-cytosine (GC) content of 28.20%. Similarly, this genome was annotated with 235 genes, including 200 protein-coding genes, 31 tRNAs, 1 tmRNA, and 3 rRNAs. Additionally, the mitochondrial genome measured 27,014 bp in length and exhibited a GC content of 27.24%. This genome was annotated with 49 genes, including 26 protein-coding genes, 21 tRNAs, and 2 rRNAs (Fig. 3C and D).

Syntenic comparison of organelle genomes between gametophyte and chantransia

A comparison of organelle genome structures revealed a high degree of homology between the chloroplast and mitochondrial genomes. The chloroplast genome of gametophyte SXU-YN24005 measured 184,899 bp, while that of chantransia SXU-YN24006 was 184,887 bp. No significant differences were observed in genome size or gene number between these genomes. Additionally, some genes exhibited minor positional variations, differing by only a few bases. Furthermore, the mitochondrial genomes measured 26,867 bp and 27,014 bp, respectively; no significant differences were observed. However, the mitochondrial genome of gametophyte SXU-YN24005 was found to lack two tRNA-Leu (tag) genes compared to that of the chantransia strain. In conclusion, the chloroplast and mitochondrial genomes of the gametophytic and chantransia stages exhibited a complete covariance structure (Fig. 4A and B). These findings align with the transcriptomics study by Fangru Nan on various life history stages of *Thorea hispida*, demonstrating that organelle genome data from the gametophyte and chantransia stages are highly similar [6].

Genome phylogenomic analysis

This study investigates 39 genes from the chloroplast genome and 10 genes from the mitochondrial genome. The Cyanidiophyceae were utilized as outgroups. A phylogenetic tree of organelle genomes was constructed employing Bayesian inference and Maximum Likelihood methods. As depicted in Fig. 5A and B, the nodes of the chloroplast and mitochondrial genomes exhibited significant support and high consistency in topology. In this analysis, the phylogenetic tree derived from the Bayesian inference served as a reference point, with support values from both methods indicated at respective positions. The phylogenetic tree of organelle genomes in endoparasites encompasses three distinct clades: Florideophyceae, Bangiophyceae, and Compsopogonophyceae. Within Florideophyceae, four divisions are identified: Rhodymeniophycidae, Corallinophycidae, Nemaliophycidae, and Hildenbrandiophycidae. Nemaliophycidae and Hildenbrandiophycidae form a unified clade, supported by strong support values (100/1.00, 99/1.00), suggesting a relatively close evolutionary relationship. In contrast, Nemaliophycidae and Hildenbrandiophycidae are recognized as distinct clades, also receiving high support values (100/1.00, 99/1.00). Additionally, Bangiophyceae and Compsopogonophyceae represent distinct clades (100/1.00, 89/1.00).

The results of this study, derived from the phylogenetic tree of organelle genomes, indicate that the gametophyte (SXU-YN24005) and chantransia (SXU-YN24006) algal strains collected from Kunming, Yunnan Province, are located within the Nemaliophycidae branch and are clustered with *Virescentia guangxiensis* from Linfen, Shanxi Province. The genetic distance between their chloroplast genomes is 0, while the nucleotide variation ranges from

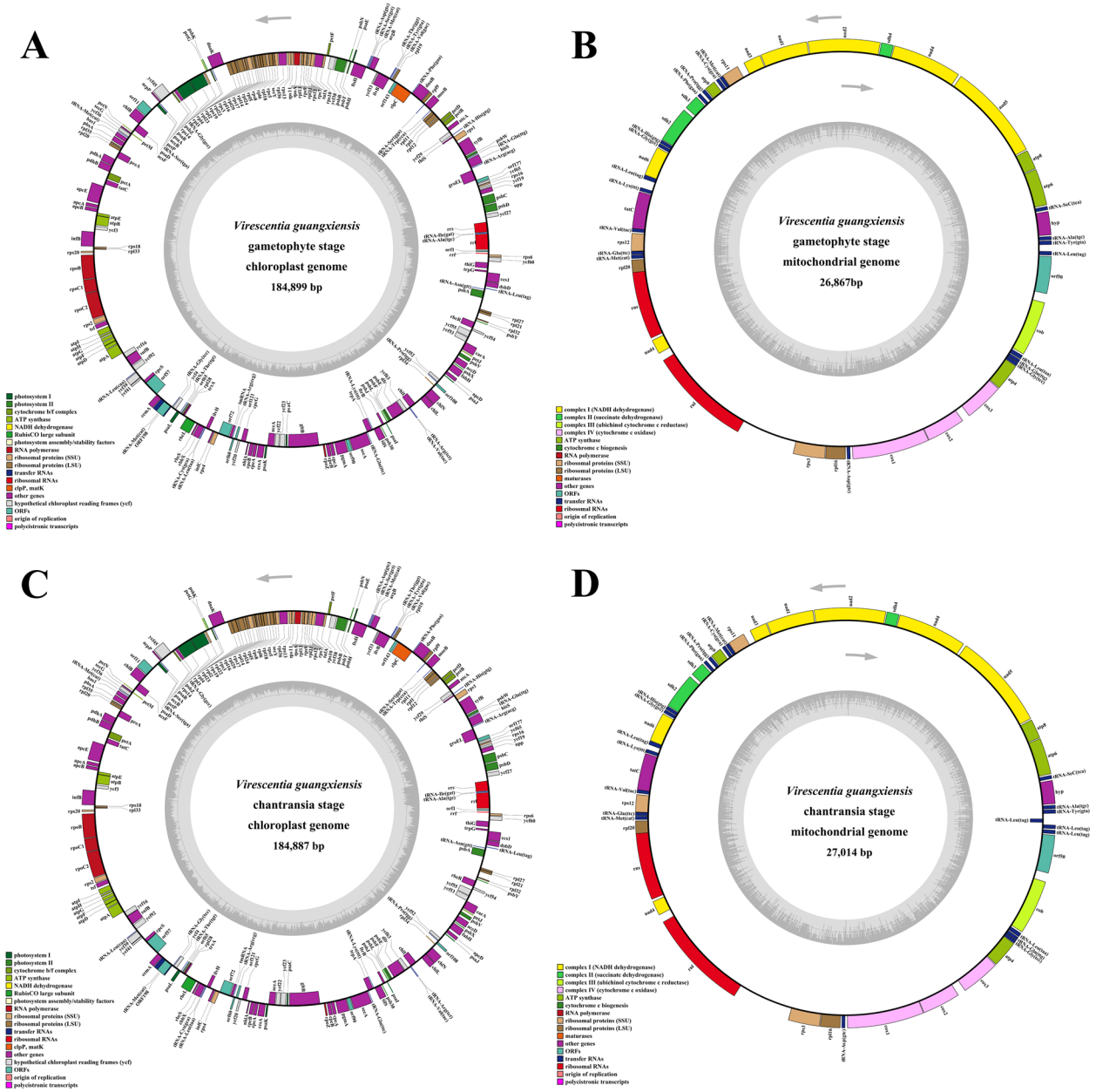

Fig. 3 Organelle genome maps of the gametophyte and chantransia specimen of *Virescentia guangxiensis*. The genes inside and outside of the circles are transcribed in the clockwise and counterclockwise directions, respectively. Genes belonging to different functional groups are shown in different colors. **A** Chloroplast genome map of the gametophyte specimen; **B** Mitochondrial genome map of the gametophyte specimen; **C** Chloroplast genome map of the chantransia specimen; **D** Mitochondrial genome map of the chantransia specimen

48 to 51 bp. The genetic distance in their mitochondrial genomes is 1%, along with a nucleotide variation of 80 to 81 bp. This clustering received robust support (100/1.00). Hence, it can be inferred that the gametophyte (SXU-YN24005) and chantransia (SXU-YN24006) algal strains exhibit a close affinity with *Virescentia guangxiensis*. Genus-level analyses revealed that this branch forms a sister group with *Kumanoa*, which clusters with a larger branch comprising *Lympha*, *Sirodotia*, *Batrachospermum*, *Paralemanea*, and *Sheathia*. Collectively, these seven genera are classified within the Batrachospermales taxon. Moreover, *Thorea hispida*, situated at the base of the Nemaliophycidae branch within the Thoreales taxon and forming a mutualistic sister group with Batrachospermales, also received robust support (100/1.00).

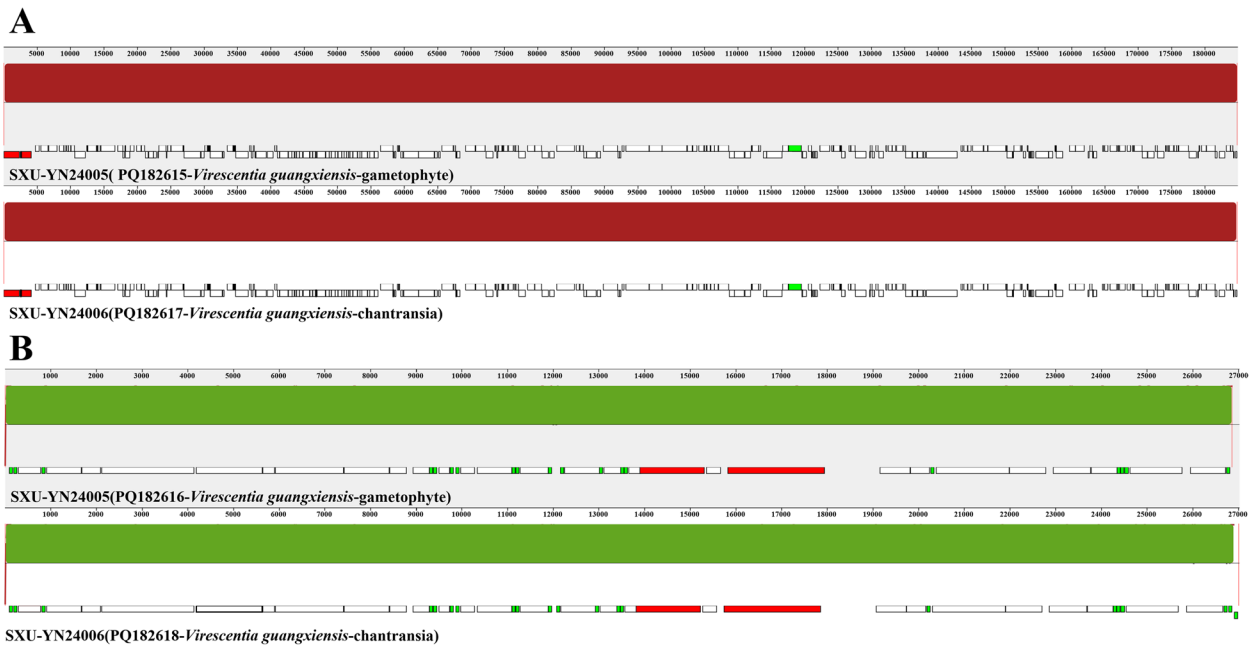

Fig. 4 Synteny alignment of organelle genomes between the gametophyte and chantransia stages of *Virescentia guangxiensis*. **A** Synteny alignment of chloroplast genomes; **B** Synteny alignment of mitochondrial genomes

Characterisatics of transcriptome data

Following the application of RNA-seq technology, raw data filtering, sequencing error rate assessment, and GC content distribution analysis were conducted. This resulted in three technical replicates of gametophyte strains, which provided clean bases of 6.67G, 6.43G, and 6.74G, with corresponding GC contents of 52.01%, 51.76%, and 51.48%. The three technical replicates of the chantransia strain provided clean bases of 6.39G, 6.41G, and 6.30G, with corresponding GC contents of 51.97%, 52.15%, and 52.10%. The sequencing data exhibited high quality (Table 2).

Transcriptomic assembly of the gametophyte and chantransia identified a total of 56,796 unigenes. Among these, unigenes with lengths ranging from 300 to 400 bp were the most abundant, exhibiting a maximum length of 9045 bp, a minimum length of 301 bp, and an average length of 712 bp. The N50 value was 838 bp, whereas the N90 value was 348 bp (Fig. 6). A BLAST search was conducted to annotate unigenes using several databases, including NR, NT, PFAM, KOG, Swiss-Prot, KEGG, and GO. The highest annotation percentage was found in the NR database (51.61%), while the lowest was in the KOG database (24%) (Fig. 7A). A total of 5179 common genes were identified across the five databases: NR, NT, KOG, GO, and PFAM (Fig. 7B). Further comparative annotation using the NR database indicated that the species with the highest number of homologous genes to the gametophyte and chantransia strain (*Virescentia guangxiensis*) included *Chondrus crispus* (9.4%), *Gracilariopsis chorda* (7.9%), *Gracilaria domingensis* (4.1%), *Coccomyxa* sp. (3.0%), and *Phaeodactylum tricornutum* (2.7%) (Fig. 7C).

The Gene Ontology (GO) annotation results were used to systematically classify all successfully annotated unigenes in this study. This resulted in the annotation of 25,084 genes across GO terms (Fig. 8A) [37]. Of these, 42,101 genes were categorized as Biological Processes, 14,458 as Cellular Components, and 30,656 as Molecular Functions. Within the Biological Processes category, the cellular process and metabolic process collectively accounted for 62.5% of the genes. In the Cellular Components category, the majority of genes (97.2%) were classified as either cellular anatomical entities or protein-containing complexes. In the Molecular Functions category, binding and catalytic activities accounted for 75.9% of the total genes.

A total of 13,632 genes were annotated in the KOG database. The four most prevalent functional categories are translation, ribosomal structure and biogenesis, post-translational modification, protein turnover, chaperones, and general function prediction. Collectively, these categories account for 52.7% of the total entries in the database (Fig. 8B).

In this study, the annotated genes were classified according to their involvement in KEGG metabolic pathways, totaling 33,022 genes distributed across 28 pathways in seven categories (Fig. 8C). The pathways with the largest numbers of annotated genes are

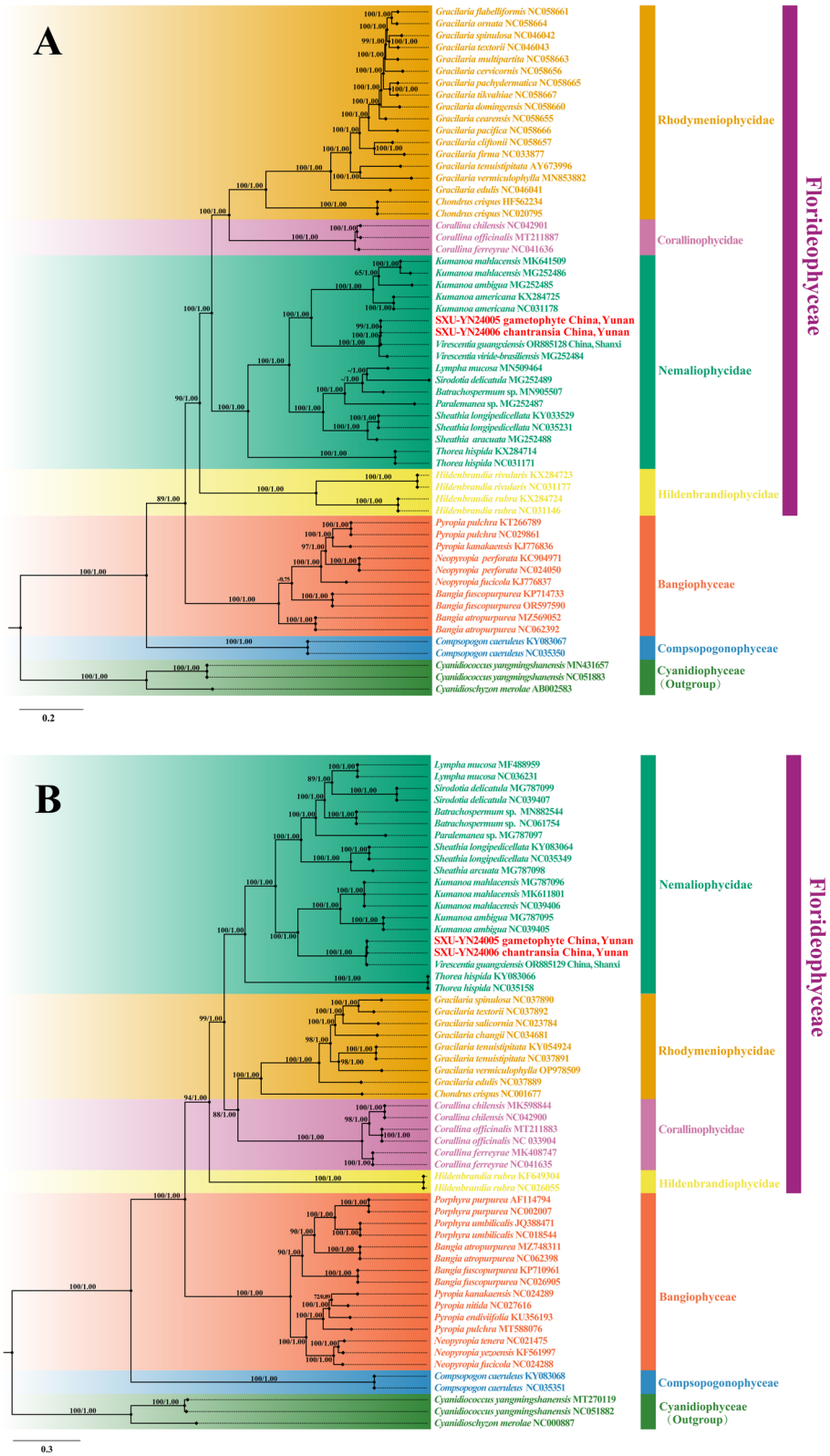

Fig. 5 Bayesian phylogenetic tree based on organelle genomes. The support is shown below: ML bootstrap/Bayesian posterior probabilities. "–" indicates that the two tree topologies at the node are inconsistent. **A** Bayesian phylogenetic tree based on chloroplast genome; **B** Bayesian phylogenetic trees based on mitochondrial genome

Table 2 Sequencing results of the transcriptome data for different life history stages of *Virescentia guangxiensis*

Sample	Raw reads	Clean reads	Raw bases	Clean bases	Error (%)	Q20 (%)	Q30 (%)	GC content (%)
Gametophyte 1	22,971,168	22,226,878	6.89G	6.67G	0.01	99.07	97.18	52.01
Gametophyte 2	21,992,942	21,436,159	6.60G	6.43G	0.01	98.99	96.94	51.76
Gametophyte 3	22,958,589	22,478,874	6.89G	6.74G	0.01	98.37	95.40	51.48
Chantransia 1	21,762,510	21,286,840	6.53G	6.39G	0.01	99.12	97.35	51.97
Chantransia 2	21,885,233	21,358,560	6.57G	6.41G	0.01	99.13	97.38	52.15
Chantransia 3	21,598,846	20,999,408	6.48G	6.30G	0.01	99.20	97.59	52.10

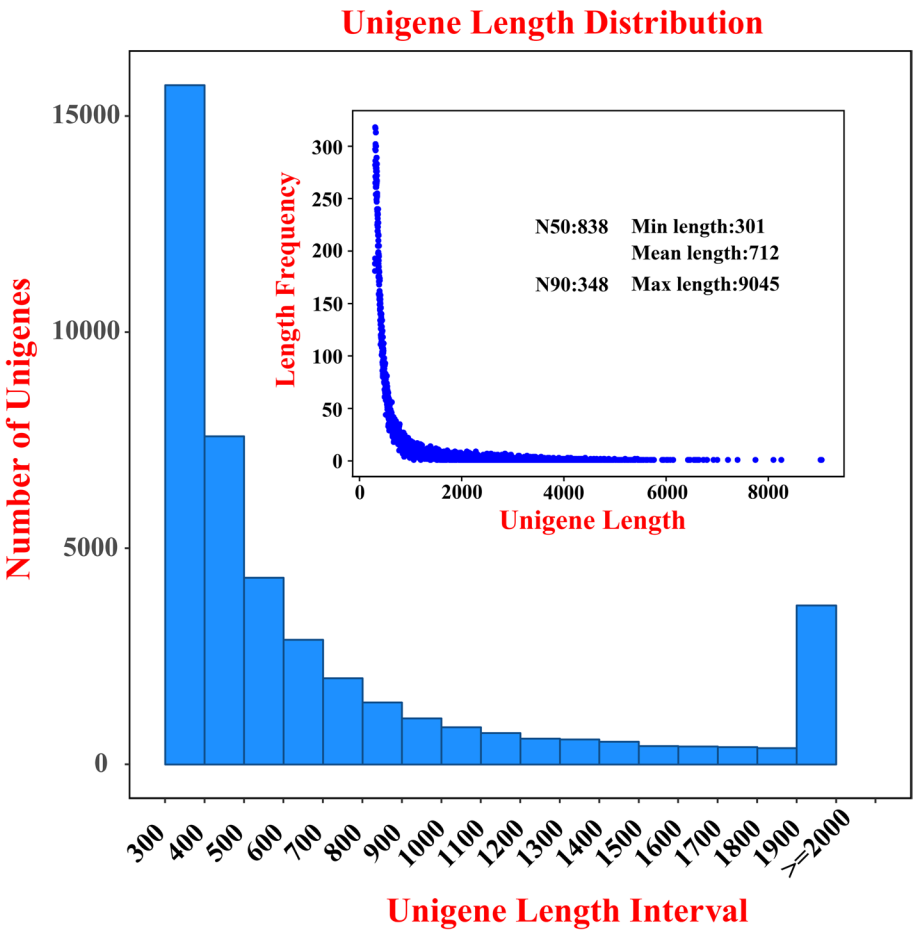

Fig. 6 Annotated unigene-bar from clean reads of *Virescentia guangxiensis*

(a) brite hierarchies, comprising 16,701 genes (50.58% of the total), (e) metabolism, comprising 7934 genes (24.03% of the total), (d) genetic information processing: 5611 genes (16.99% of the total), (b) cellular processes: 1210 genes (3.66% of the total). (f) not included in a pathway or brite: 700 genes (2.12% of the total). (c) environmental information processing: 578 genes (1.75% of the total). (g) organismal systems: 288 genes (0.87% of the total).

Comparison of transcriptome for two life history stages

This study aimed to elucidate the transcriptional patterns of specific genes in the gametophyte and chantransia stages of *Virescentia guangxiensis* (Fig. 9A and B). The FPKM (Fragments Per Kilobase of transcript per Million base pairs) method was employed to assess discrepancies in expression distribution between samples. Figure 9A illustrates notable discrepancies in the density values of genes with identical expression levels between

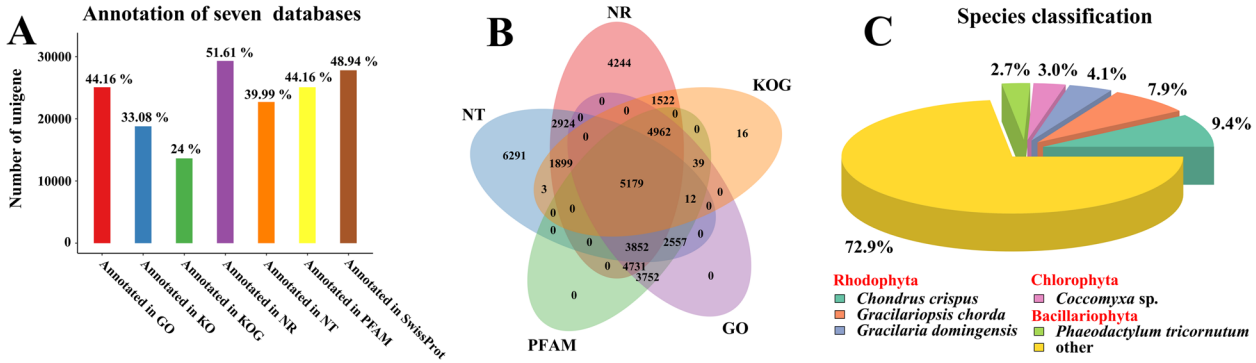

Fig. 7 Function annotations of unigenes of *Virescentia guangxiensis* based on blast against diverse databases. **A** Numbers of unigenes annotated in seven databases; **B** Venn diagram of unigenes annotated in five databases; **C** Classification of species with gene homology to *Virescentia guangxiensis* based on NR annotion result

the gametophyte and chantransia stages. Moreover, the volcano plots offer a visual representation of the statistical significance of differences in gene expression across the two life history stages. Figure 9B reveals that 2390 up-regulated genes and 8498 down-regulated genes were identified in the gametophyte stage compared to the chantransia stage. This finding indicates notable differences in gene expression patterns between the two life history stages, potentially reflecting their distinct physiological and ecological adaptations.

The most significantly down-regulated genes enriched in KEGG pathways at the gametophyte stage, compared to the chantransia stage, included those involved in ribosome pathways. Following these were pathways associated with Photosynthesis—antenna proteins, photosynthesis, and Carbon fixation in photosynthetic organisms (Fig. 10). Utilizing the transcriptome database, a comparison of |log2(FoldChange)| and adjusted *p*-values (padj) identified three specific photosynthesis-related genes: LHCA1, *psb*O, and *rbc*S, as well as the gene S17e, which encodes the ribosomal 40S subunit protein. All identified genes were significantly down-regulated (Fig. S2). Moreover, the qRT-PCR results were consistent with the findings from the transcriptome sequencing. Quantitative comparisons of the selected four genes between the gametophyte and chantransia stages were conducted (Fig. 11).

Discussion

Both Batrachospermales and Thoreales exhibit a three-phase alternating life history of generations, that includes a gametophyte stage, a carposporophyte attached to the gametophyte, and chantransia capable of asexual reproduction via monosporangia [4, 38]. Notable morphological distinctions exist between the gametophyte and chantransia in the Batrachospermales taxon. However, chantransia are morphologically similar to those in the genus *Audouinella* of the family Acrochaetiales. This similarity may cause confusion between the two groups, presenting a significant challenge for accurate taxonomic identification. A phylogenetic tree constructed using the *rbc*L and COI-5P genes indicated that the samples from this study clustered with *Virescentia guangxiensis*, achieving strong support (not shown). Subsequent phylogenetic analyses of the chloroplast and mitochondrial genomes yielded identical results, supporting the hypothesis that the chantransia and gametophyte strains from this study represent a single species, *Virescentia guangxiensis*. This study is the first to collect algal strains from different life history stages simultaneously at the same site. This study observed that chantransia strains were abundant on the stone wall adjacent to the spring, while gametophyte strains were attached to the chantransia strains in lower quantities.

The genetic distance between the chloroplast and mitochondrial genomes was 0 in both the gametophyte and chantransia stages, indicating nucleotide variations of 9–15 bp. The chloroplast genomes of the two stages exhibited complete identity in gene number, with gene locations nearly identical and only a 12 bp difference in gene size. In the mitochondrial genome, gene positions were approximately the same. Nevertheless, there is a 147 bp size difference among these genomes. When compared with the chantransia strain, the mitochondrial genome of the gametophyte strain is lacking two tRNA-Leu(tag) genes. In conclusion, a covariance comparison of organelle genomes from different life-history stages demonstrates substantial homology and a high degree of conservation in their sequences. This finding is consistent with previous studies [39–42]. The growing number of freshwater red algal samples has resulted in the identification of additional intermediate forms. This has created

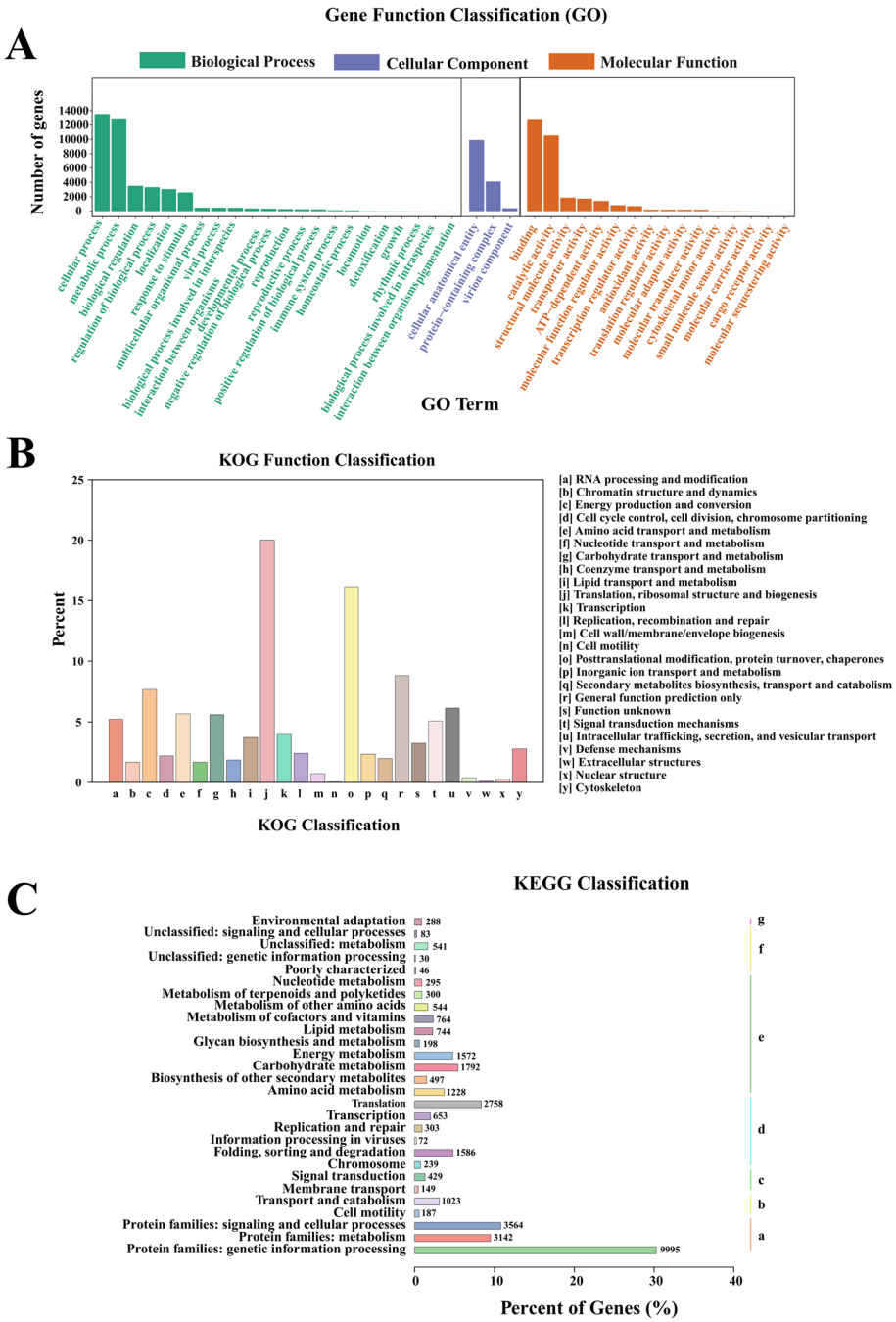

Fig. 8 Gene function classification based on different databases for the predicted unigenes. **A** Gene function classification according to GO assignments for the predicted *Virescentia guangxiensis* unigenes; **B** Gene function classification according to KOG assignments for the predicted *Virescentia guangxiensis* unigenes; **C** The biological pathways in *Virescentia guangxiensis* according to the Kyoto Encyclopedia of Genes and Genomes (KEGG) database; a represents brite hierarchies; b represents cellular processes; c. represents environmental information processing; d represents genetic information processing; e represents metabolism; f represents not included in pathway or brite; g represents organismal systems. Number on the right margin of each bar represents of unigenes in the corresponding subcategories

a demand for more sophisticated phylogenetic classification methods to address the observed diversity in these samples. Consequently, utilizing organelle genomic and transcriptomic data to elucidate phylogenetic relationships has emerged as a significant trend in contemporary research.

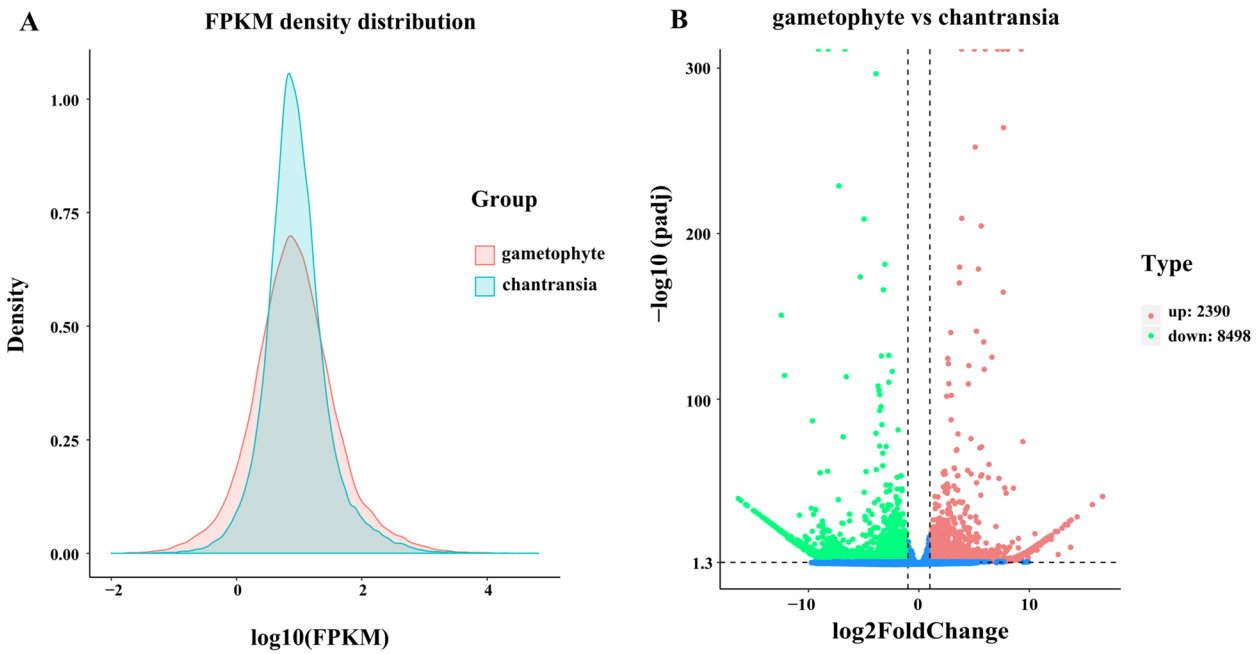

Fig. 9 Different gene transcriptional patterns for the gametophyte and chantransia stages of *Virescentia guangxiensis*. **A** FPKM (Fragments Per Kilobase per Million mapped reads) density distribution for the gametophyte and chantransia stages of *Virescentia guangxiensis*; **B** Volcanoplot showing the up and down regulated genes for the gametophyte and chantransia stages of *Virescentia guangxiensis*

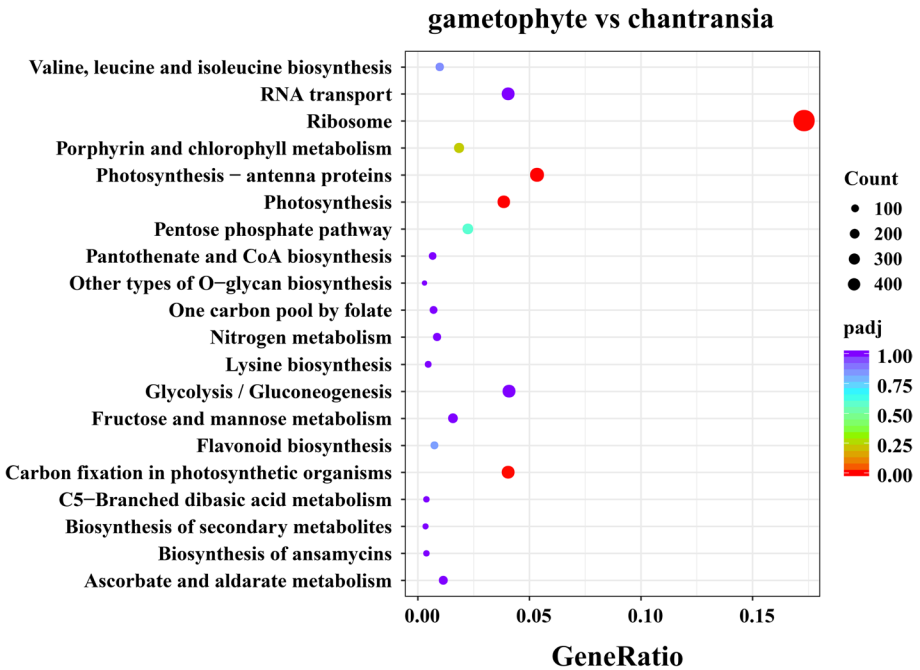

Fig. 10 Enriched KEGG pathway for down regulated genes for the gametophyte and chantransia stages of *Virescentia guangxiensis*

This study revealed that genes associated with photosynthesis and ribosomes experienced a significant decline in expression during the gametophyte stage compared to the chantransia stage. This finding contradicts observations made by Fangru Nan in her study of various life-history stages of *Thorea hispida* [6]. Samples of the gametophyte and chantransia from *Thorea hispida* were collected at different times (April 9 and June 18).

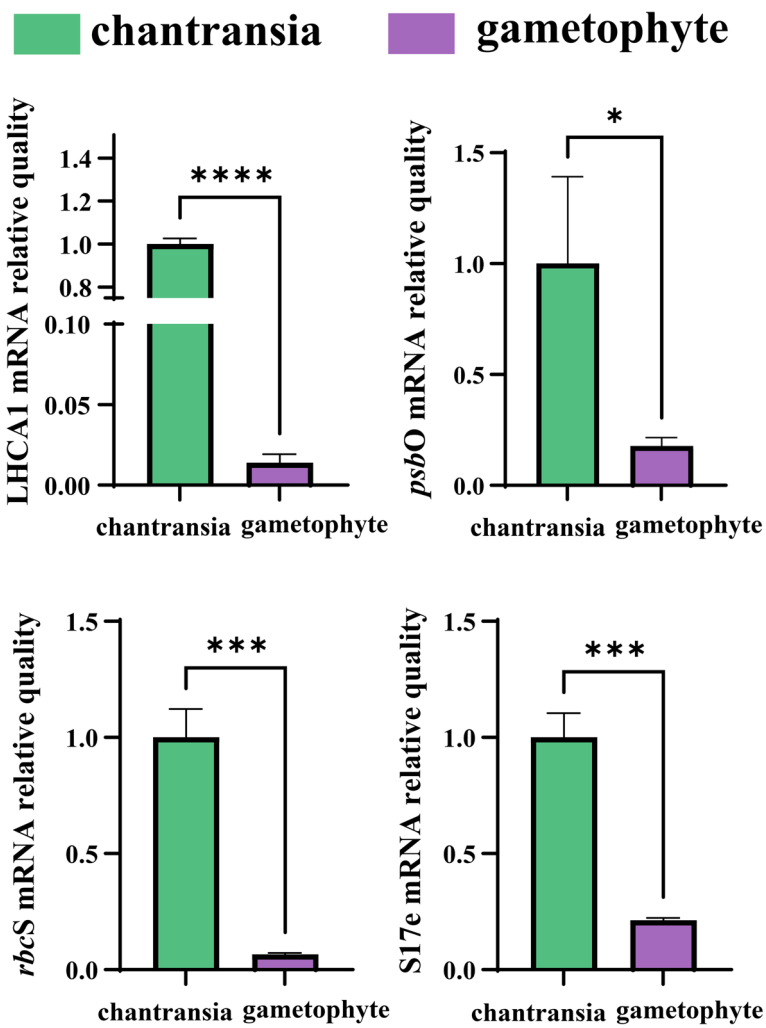

Fig. 11 Gene expression in the gametophyte and Chantransia specimens was validated using qRT-PCR. The qRT-PCR results demonstrated that 'mRNA relative quality' is quantified as 2-ΔΔCt. * 0.1 level of significance; ** 0.05 level of significance; *** 0.001 level of significance; **** 0.0001 level of significance

Furthermore, samples of *Thorea hispida* were exposed to natural light, while samples in this study were collected from a spring pool where vegetables are washed daily and covered by an artificial shade canopy. Consequently, the plants experienced more heterogeneous light conditions than those of *Thorea hispida*.

Previous studies have shown that taxa in the Batrachospermales typically thrive in low-light conditions, consistent with the habitat of the collected *Virescentia* [4, 43]. Transcriptome data indicated that gametophyte preferred lower light levels for growth compared to chantransia under identical habitat conditions, whereas chantransia had a relatively high photosynthetic capacity.

During the gametophyte stage, genes encoding the photosynthesis-antennal protein pathway, specifically LHCA1, LHCA3, LHCA4, LHCA5, LHCB1, LHCB2, LHCB3, LHCB4, LHCB5, and LHCB6, associated with the synthesis of phototropic pigment proteins in PS I, showed a significant decline in expression compared to the chantransia stage [44, 45]. The main site for oxygen release during photosynthesis is PS II, which facilitates this process via protein complexes. In contrast, the expression of the *cpc*B gene was significantly upregulated. Along with the *cpc*A gene, it synthesizes deocofactor phycocyanin, which primarily facilitates the biosynthesis of optically active phycobiliproteins [46]. Genes such as *psb*O, *psb*P, *psb*Q, *psb*R, *psa*F, *psa*K, *psa*L, and *psa*O exhibited a significant decline in expression within the photosynthetic electron transport chain during the gametophyte stage. Among these, *psb*O, *psb*P, *psb*Q, and *psb*R regulate calcium and chloride ions and are involved in synthesizing the photosynthetic oxygen-evolving protein complex of PS II [47, 48]. In 2007, it was demonstrated that the *psa*F gene, which encodes the

systemic subunit III of PS I, is regulated by Ca^{2+} responsive kinases and phosphatidylinositol signaling intermediates [49]. Furthermore, genes such as *psa*K, *psa*L, and *psa*O play a critical role in stabilizing the PS I reaction center, participating in electron transfer, and synergizing with LHCI [49]. The *rbc*L and *rbc*S genes, associated with CO_2 fixation, encode the large and small subunits of ribulose-1,5-bisphosphate carboxylase/oxygenase, respectively. These enzymes are essential for catalyzing the reaction that fixes CO_2 [50]. The expression of genes such as *rbc*L, *rbc*S, and *rpe* is significantly reduced during the gametophyte stage, suggesting in a reduced photosynthetic rate. The ribosome is the organelle responsible for catalyzing protein synthesis within cells. It consists of a small 40S subunit and a large 60S subunit [51]. Ribosome-related genes, such as S17e, S4e, S3Ae, L4e, LP0, and L40e, are significantly down-regulated during the gametophyte stage, while only the RPS2 gene was significantly up-regulated. These genes are involved in ribosome assembly and structural maintenance, as well as in the initiation, elongation, and termination of protein synthesis. Overall, photosynthesis significantly influences gene expression at various life history stages [52].

Conclusions

(1) This study utilized phylogenetic analysis of the chloroplast and mitochondrial genomes to confirm that the sample from Leju Village, Kunming City, Yunnan Province, is *Virescentia guangxiensis*. Notably, this is the first instance in which two samples of the same species at different life history stages were collected simultaneously from the same location.

(2) Comparative covariance analysis revealed that the chloroplast and mitochondrial genomes are highly conserved in both gametophyte and chantransia stages, supporting the stability of the algal genome across various life history stages.

(3) Transcriptome sequencing revealed significant differences in gene expression patterns between the two life history stages. Gene expression associated with photosynthesis and ribosomes was significantly reduced in the gametophyte stage compared to the chantransia stage. Under optimal low-light conditions, gametophyte demonstrated a greater ability to adapt to low light than the chantransia stage, which showed a higher photosynthetic capacity. A detailed examination of the sampled habitats indicated that gametophyte strains were attached to chantransia strains, which were extensively distributed around them. We speculate that the distinct survival patterns of gametophytes and chantransia may influence gene expression. Nonetheless, the underlying mechanisms necessitate further investigation.

Supplementary Information

The online version contains supplementary material available at https://doi.org/10.1186/s12864-025-11396-1.

Supplementary Material 1: Fig. S1. Map of China showing the location of the study area Leju Village, Kunming City,Yunnan Province, China. Fig. S2. Heatmap of the correlation of four significantly different genes screened in the KEGG pathway. Table S1. Chloroplast genome information. Table S1. Mitochondrial genome information.

Acknowledgements
We gratefully acknowledge Fangru Nan and Qi Liu for their assistance in collecting samples for this study.

Authors' contributions
W.G. and S.X. designed the study, interpreted all the data and findings and wrote the manuscript, and made equal contributions as major authors. F.N., X.L., Q.L. and J. F. validated, revised, and edited the final manuscript. All authors have read and agreed to the published version of the manuscript.

Funding
This work was funded by the National Natural Science Foundation of China (grant number 32170204).

Data availability
Data is provided within the manuscript.

Declarations

Ethics approval and consent to participate
Our materials were collected from Leju Village, Kunming, Yunnan Province, China. No specifc permits are required for sample collection in this study. We comply with relevant institutional, national and international guidelines and legislation for study.

Consent for publication
Not applicable.

Competing interests
The authors declare no competing interests.

Received: 7 January 2025 Accepted: 21 February 2025
Published online: 27 February 2025

References

1. Xie SL. Seasonal dynamics of *Batrachospermum arcuatum* growth and distribution in Jinci Spring China. J Shanxi Univ. 2009;32(4):596–600 (in Chinese).
2. Szinte AL, Taylor JC, Abosede AT, Vis ML. Current status of freshwater red algal diversity (Rhodophyta) of the African continent including description of new taxa (Batrachospermales). Phycologia. 2020;59(3):187–99.
3. Vis ML, Necchi O Jr. Subphylum Eurhodophytina, Class Florideophyceae, Subclass Nemaliophycidae, Order Batrachospermales. In: Freshwater red algae Phylogeny, taxonomy and biogeography. Springer Nature Switzerland AG, Cham: International Publishing; 2021. p. 129–323.
4. Shi ZX, Xie SL, Hua D. Flora Algarum Sinicarum Aquae Dulci, Tomus XIII, Rhodophyta, Phaeophyta. Beijing: Science Press, 2006; pp.1–77. (in Chinese).

5. Nan FR, Feng J, Lv JP, Liu Q, Xie SL. Transcriptome analysis of the typical freshwater rhodophytes *Sheathia arcuata* grown under different light intensities. PLoS ONE. 2018;13(5): e0197729.
6. Nan FR, Feng J, Lv JP, Liu Q, Liu XD, Gao F, Xie SL. Comparison of the transcriptomes of different life history stages of the freshwater Rhodophyte *Thorea hispida*. Genomics. 2020;112(6):3978–90.
7. Saunders GW. Gel purifi cation of red algal genomic DNA an inexpensive and rapid method for the isolation of polymerase chain reaction-friendly DNA. J Phycol. 1993;29(2):251–4.
8. Vis ML, Sheath RG. Biogeography of *Batrachospermum gelatinosum* (Batrachospermales, Rhodophyta) in North America based on molecular and morphological data. J Phycol. 1997;33(3):520–6.
9. Cock PJA, Fields CJ, Goto N, Heuer ML, Rice PM. The Sanger FASTQ file format for sequences with quality scores, and the Solexa/Illumina FASTQ variants. Nucleic Acids Res. 2010;38(6):1767–71.
10. Jiang LC, Schlesinger F, Davis CA, Zhang Y, Li RH, Salit M, Gingeras TR, Oliver B. Synthetic spike-in standards for RNA-seq experiments. Genome Res. 2011;21(9):1543–51.
11. Yan LY, Yang MY, Guo HS, Yang L, Wu J, Li R, Liu P, Lian Y, Zheng XY, Yan J, Huang J, Li M, Wu XL, Wen L, Lao KQ, Li RQ, Qiao J, Tang FC. Single-cell RNA-Seq profiling of human preimplantation embryos and embryonic stem cells. Nat Struct Mol Biol. 2013;20(9):1131–9.
12. Ruby JG, Bellare P, DeRisi JL. Price: software for the targeted assembly of components of (meta) genomic sequence data. G3 Genes|Genomes|Genetics 2013;3(5):865–880.
13. Bankevich A, Nurk S, Antipov D, Gurevich AA, Dvorkin M, Kulikov AS, Lesin VM, Nikolenko SI, Pham S, Prjibelski AD, Pyshkin AV, Sirotkin AV, Vyahhi N, Tesler G, Alekseyev MA, Pevzner PA. SPAdes: a new genome assembly algorithm and its applications to single-cell sequencing. J Comput Biol. 2012;19(5):455–77.
14. Okonechnikov K, Golosova O, Fursov M. team tU: Unipro UGENE: a unified bioinformatics toolkit. Bioinformatics. 2012;28(8):1166–7.
15. Laslett D, Canback B. ARAGORN, a program to detect tRNA genes and tmRNA genes in nucleotide sequences. Nucleic Acids Res. 2004;32(1):11–6.
16. Darling ACE, Mau B, Blattner FR, Perna NT. Mauve: multiple alignment of conserved genomic sequence with rearrangements. Genome Res. 2004;14(7):1394–403.
17. Zhang D, Gao F, Li WX, Jakovlić I, Zou H, Zhang J, Wang GT. PhyloSuite: an integrated and scalable desktop platform for streamlined molecular sequence data management and evolutionary phylogenetics studies. Mol Ecol Resour. 2020;20(1):348–55.
18. Katoh K, Standley DM. MAFFT multiple sequence alignment software v. 7: improvements in performance and usability. Mol Biol Evol. 2013;30(4):772–80.
19. Capella-Gutiérrez S, Silla-Martínez JM, Gabaldón T. trimAl: a tool for automated alignment trimming in large-scale phylogenetic analyses. Bioinformatics. 2009;25(15):1972–3.
20. Kalyaanamoorthy S, Minh BQ, Wong TKF, von Haeseler A, Jermiin LS. ModelFinder: fast model selection for accurate phylogenetic estimates. Nat Methods. 2017;14(6):587–9.
21. Nguyen LT, Schmidt HA. Haeseler Av, Minh BQ: IQ-TREE: a fast and effective stochastic algorithm for estimating maximum-likelihood phylogenies. Mol Biol Evol. 2015;32(1):268–74.
22. Ronquist F, Teslenko M, van der Mark P, Ayres DL, Darling A, Hohna S, Larget B, Liu L, Suchard MA, Huelsenbeck JP. MrBayes 3.2: efficient Bayesian phylogenetic inference and model choice across a large model space. Syst Biol. 2012;61(3):539–42.
23. Holmes DS, Bonner J. Preparation, molecular weight, base composition, and secondary structure of giant nuclear ribonucleic acid. Biochemistry. 1973;12(12):2330–8.
24. Grabherr MG, Haas BJ, Yassour M, Levin JZ, Thompson DA, Amit I, Adiconis X, Fan L, Raychowdhury R, Zeng QD, Chen ZH, Mauceli E, Hacohen N, Gnirke A, Rhind N. Palma Fd, Birren BW, Nusbaum C, Lindblad-Toh K, Friedman N, Regev A: Full-length transcriptome assembly from RNA-Seq data without a reference genome. Nat Biotechnol. 2011;29(7):644–52.
25. Davidson NM, Oshlack A. Corset: enabling differential gene expression analysis for de novo assembled transcriptomes. Genome Biol. 2014;15(7):410.
26. Buchfink B, Xie C, Huson DH. Fast and sensitive protein alignment using DIAMOND. Nat Methods. 2015;12(1):59–60.
27. Altschul SF, Madden TL, Schäffer AA, Zhang JH, Zhang Z, Miller W, Lipman DJ. Gapped BLAST and PSI-BLAST: a new generation of protein database search programs. Nucleic Acids Res. 1997;25(17):3389–402.
28. Moriya Y, Itoh M, Okuda S, Yoshizawa AC, Kanehisa M. KAAS: an automatic genome annotation and pathway reconstruction server. Nucleic Acids Res. 2007;35(suppl_2, 1):W182-W185.
29. Götz S, García-Gómez JM, Terol J, Williams TD, Nagaraj SH, Nueda MJ, Robles M, Talón M, Dopazo J, Conesa A. High-throughput functional annotation and data mining with the Blast2GO suite. Nucleic Acids Res. 2008;36(10):3420–35.
30. Eddy SR. Accelerated profile HMM searches. PLoS Comput Biol. 2011;7(10): e1002195.
31. Finn RD, Bateman A, Clements J, Coggill P, Eberhardt RY, Eddy SR, Heger A, Hetherington K, Holm L, Mistry J, et al. Pfam: the protein families database. Nucleic Acids Res. 2014;42(D1):D222–30.
32. Li B, Dewey CN. RSEM: accurate transcript quantification from RNA-Seq data with or without a reference genome. BMC Bioinf. 2011;12(323):1–16.
33. Robinson MD, McCarthy DJ, Smyth GK. edgeR: a Bioconductor package for differential expression analysis of digital gene expression data. Bioinformatics. 2010;26(1):139–40.
34. Young MD, Wakefield MJ, Smyth GK, Oshlack A. Gene ontology analysis for RNA-seq: accounting for selection bias. Genome Biol. 2010;11(2: R14):1–12.
35. Kanehisa M, Araki M, Goto S, Hattori M, Hirakawa M, Itoh M, Katayama T, Kawashima S, Okuda S, Tokimatsu T, Yamanishi Y. KEGG for linking genomes to life and the environment. Nucleic Acids Res. 2008;36(suppl_1):D480-D484.
36. Mao XZ, Cai T, Olyarchuk JG, Wei LP. Automated genome annotation and pathway identification using the KEGG Orthology (KO) as a controlled vocabulary. Bioinformatics. 2005;21(19):3787–93.
37. Ashburner M, Ball CA, Blake JA, Botstein D, Butler H, Cherry JM, Davis AP, Dolinski K, Dwight SS, Eppig JT, Harris MA, Hill DP, Issel-Tarver L, Kasarskis A, Lewis S, Matese JC, Richardson JE, Ringwald M, Rubin GM, Gavin S. Gene Ontology: tool for the unification of biology. Nat Genet. 2000;25(1):25–9.
38. Sheath RG. The biology of freshwater red algae. UK: Biopress Ltd, Bristol; 1984.
39. Yang EC, Kim KM, Kim SY, Lee J, Boo GH, Lee J-H, Nelson WA, Yi G, Schmidt WE, Fredericq S, Boo SM, Bhattacharya D, Yoon HS. Highly conserved mitochondrial genomes among multicellular red algae of the Florideophyceae. Genome Biol Evol. 2015;7(8):2394–406.
40. Lee J, Cho CH, Park SI, Choi JW, Song HS, West JA, Bhattacharya D, Yoon HS. Parallel evolution of highly conserved plastid genome architecture in red seaweeds and seed plants. BMC Biol. 2016;14:1–16.
41. Paiano MO, Del Cortona A, Costa JF, Liu SL, Verbruggen H, De Clerck O, Necchi O Jr. Organization of plastid genomes in the freshwater red algal order Batrachospermales (Rhodophyta). J Phycol. 2018;54(1):25–33.
42. Wolf DI, Evans JR, Vis ML. Complete mitochondrial genome of the freshwater red alga *Lympha mucosa* (Rhodophyta). Mitochondrial DNA B Resour. 2017;2(2):707–8.
43. Necchi O Jr. Light-related photosynthetic characteristics of freshwater rhodophytes. Aquat Bot. 2005;82(3):193–209.
44. Milena M, Manuela M, Francesca P, Stefano C, Roberta C, Roberto B. Functional analysis of Photosystem I light-harvesting complexes (Lhca) gene products of *Chlamydomonas reinhardtii*. Biochim Biophys Acta Bioenerg. 2010;1797(2):212–21.
45. Crepin A, Caffarri S. Functions and evolution of Lhcb isoforms composing LHCII, the major light harvesting complex of photosystem II of green eukaryotic organisms. Curr Protein Pept Sci. 2018;19(7):699–713.
46. Teneva I, Stoyanov P, Mladenov R, Dzhambazov B. Molecular and phylogenetic characterization of two species of the genus *Nostoc* (Cyanobacteria) based on the *cpcB-IGS-cpcA* locus of the phycocyanin operon. J BioSci Biotech. 2012;1(1):9–19.
47. Miqyass M, van Gorkom HJ, Yocum CF. The PSII calcium site revisited. Photosynth Res. 2007;92(3):275–87.
48. Bricker TM, Frankel LK. Auxiliary functions of the PsbO, PsbP and PsbQ proteins of higher plant Photosystem II: A critical analysis. J Photochem Photobiol B. 2011;104(1–2):165–78.
49. Vanselow C, Weber APM, Krause K, Fromme P. Genetic analysis of the Photosystem I subunits from the red alga. Galdieria sulphuraria Biochim Biophys Acta Bioenerg. 2009;1787(1):46–59.

50. Freshwater DW, Fredericq S, Butler BS, Chase MW. A gene phylogeny of the red algae (Rhodophyta) based on plastid *rbc*L. Proc Natl Acad Sci U S A. 1994;91(15):7281–5.
51. Eisinger DP, Dick FA, Trumpower BL. Qsr1p, a 60S ribosomal subunit protein, is required for joining of 40S and 60S subunits. Mol Cell Biol. 1997;17(9):5136–45.
52. Ying X, Chen W, Chen Q, Zhang X, Xu N, Sun X. Differences between the wild-type and cultivated *Gracilariopsis lemaneiformis* revealed by quantitative proteome and gene expression profiling analysis. Bot Mar. 2023;66(5):437–51.

Publisher's Note